

LONDON  
SCHOOL of  
HYGIENE  
& TROPICAL  
MEDICINE



LSHTM Research Online

Bhalla, Manmeet; Hoan, Van Ngo; Gyanwali, Gaurav Chandra; Iretona, Keith; (2018) The Host Scaffolding Protein Filamin A and the Exocyst Complex Control Exocytosis during InlB-Mediated Entry of *Listeria monocytogenes*. *INFECTION AND IMMUNITY*, 87 (1). ISSN 0019-9567 DOI: <https://doi.org/10.1128/IAI.00689-18>

Downloaded from: <http://researchonline.lshtm.ac.uk/4651595/>

DOI: <https://doi.org/10.1128/IAI.00689-18>

**Usage Guidelines:**

Please refer to usage guidelines at <https://researchonline.lshtm.ac.uk/policies.html> or alternatively contact [researchonline@lshtm.ac.uk](mailto:researchonline@lshtm.ac.uk).

Available under license: <http://creativecommons.org/licenses/by-nc-nd/2.5/>

<https://researchonline.lshtm.ac.uk>

1

2 The host scaffolding protein Filamin A and the exocyst complex  
3 control exocytosis during InlB-mediated entry of  
4 *Listeria monocytogenes*

5

6 Manmeet Bhalla<sup>a</sup>, Hoan Van Ngo<sup>a,b</sup>, Gaurav Chandra Gyanwali<sup>a</sup>, and Keith Ireton<sup>a,\*</sup>

7 <sup>a</sup> Department of Microbiology and Immunology, University of Otago, Dunedin, New  
8 Zealand

9 <sup>b</sup> Present address: Department of Immunology and Infection, Faculty of Infectious  
10 and Tropical Diseases, London School of Hygiene and Tropical Medicine, London,  
11 United Kingdom.

12

13 \* Address correspondence to Keith Ireton, [keith.ireton@otago.ac.nz](mailto:keith.ireton@otago.ac.nz).

14

15 Running title:

16 Control of host exocytosis during InlB-mediated entry

17

18  
19  
20  
21  
22  
23  
24  
25  
26  
27  
28  
29  
30  
31  
32  
33  
34  
35  
36  
37  
38  
39  
40

## SUMMARY

*Listeria monocytogenes* is a food-borne bacterium that causes gastroenteritis, meningitis, or abortion. *Listeria* induces its internalization (entry) into some human cells through interaction of the bacterial surface protein InlB with its host receptor, the Met tyrosine kinase. InlB and Met promote entry, in part, through stimulation of localized exocytosis. How exocytosis is upregulated during entry is not understood. Here we show that the human signaling proteins mTOR, Protein Kinase C (PKC)- $\alpha$ , and RalA promote exocytosis during entry by controlling the scaffolding protein Filamin A (FlnA). InlB-mediated uptake was accompanied by PKC- $\alpha$  –dependent phosphorylation of serine 2152 in FlnA. Depletion of FlnA by RNA interference (RNAi) or expression of a mutated FlnA protein defective in phosphorylation impaired InlB-dependent internalization. These findings indicate that phosphorylation of FlnA by PKC- $\alpha$  contributes to entry. mTOR and RalA were found to mediate the recruitment of FlnA to sites of InlB-mediated entry. Depletion of PKC- $\alpha$ , mTOR, or FlnA each reduced exocytosis during InlB-mediated uptake. Because the exocyst complex is known to mediate polarized exocytosis, we examined if PKC- $\alpha$ , mTOR, RalA, or FlnA affect this complex. Depletion of PKC- $\alpha$ , mTOR, RalA, or FlnA impaired recruitment of the exocyst component Exo70 to sites of InlB-mediated entry. Experiments involving knockdown of Exo70 or other exocyst proteins demonstrated an important role for the exocyst complex in uptake of *Listeria*. Collectively, our results indicate that PKC- $\alpha$ , mTOR, RalA, and FlnA comprise a signaling pathway that mobilizes the exocyst complex to promote infection by *Listeria*.

## INTRODUCTION

41

42 *Listeria monocytogenes* is a food-borne bacterium that causes gastroenteritis,  
43 meningitis or abortion (1). Critical for disease is the ability of *Listeria* to induce its  
44 internalization (entry) into nonphagocytic cells in the intestine, liver, or placenta (2).  
45 A major pathway of *Listeria* entry is mediated by binding of the bacterial surface  
46 protein InlB to its host receptor, the Met tyrosine kinase (3). Binding of InlB activates  
47 Met, resulting in the stimulation of two host processes that promote bacterial uptake:  
48 actin polymerization and exocytosis (4-6).

49

Actin polymerization is thought to contribute to entry of *Listeria* by providing  
50 a protrusive force that drives the host plasma membrane around adherent bacteria (4,  
51 7). Exocytosis is the fusion of intracellular vesicles with the plasma membrane (8).  
52 How membrane flow through exocytosis controls InlB-dependent uptake is not fully  
53 understood. One potential mechanism involves the delivery of the GTPase Dynamin 2  
54 to the host plasma membrane (6). During InlB-mediated entry, Dynamin 2  
55 translocates from an internal membrane compartment termed the recycling endosome  
56 (RE) to sites in the plasmalemma near adherent bacteria. Dynamin 2 is known to  
57 remodel membranes through a GTP-dependent scission activity and also through  
58 interaction with membrane sculpting proteins containing BAR domains (9). These  
59 membrane remodeling activities of Dynamin 2 are likely responsible for its role in  
60 InlB-mediated entry (6, 10).

61

How are actin polymerization and exocytosis stimulated during InlB-  
62 dependent uptake of *Listeria*? Substantial progress has been made on the mechanism  
63 of actin polymerization, revealing that this process is mediated by the host Arp2/3  
64 complex and the nucleation promoting factors N-WASP and WAVE (5, 11, 12). By  
65 contrast, little is known about how exocytosis is induced during InlB-mediated

66 internalization, except that induction requires the kinase activity of Met and the host  
67 GTPase RalA (6).

68 Previous results demonstrated that the human serine/threonine kinases mTOR  
69 and Protein Kinase C- $\alpha$  (PKC- $\alpha$ ) are activated downstream of Met and play important  
70 roles in InlB-mediated entry of *Listeria* (13). mTOR and PKC- $\alpha$  comprise a signaling  
71 pathway involved in several biological events, including cell migration and survival  
72 (14, 15). mTOR forms part of a multi-component complex called mTORC2 that  
73 phosphorylates serine 657 in a hydrophobic motif in PKC- $\alpha$ , thereby upregulating  
74 PKC kinase activity (16). Importantly, InlB-mediated entry of *Listeria* is  
75 accompanied by mTOR-dependent phosphorylation of serine 657 in PKC- $\alpha$ ,  
76 indicating that mTOR functions upstream of PKC- $\alpha$  during entry (13). How mTOR  
77 and PKC- $\alpha$  control internalization of *Listeria* is not well understood. Although PKC-  
78  $\alpha$  has a minor role in actin polymerization during entry, mTOR has no detectable  
79 effect on this process (13). It therefore seems likely that mTOR and PKC- $\alpha$  affect  
80 uptake of *Listeria* by regulating host processes apart from the assembly of actin  
81 filaments. One such process could be exocytosis.

82 In this work, we show that mTOR and PKC- $\alpha$  promote exocytosis during  
83 InlB-mediated entry of *Listeria* by controlling the human scaffolding protein Filamin  
84 A (FlnA). InlB-dependent internalization was accompanied by an increase in  
85 phosphorylation of serine 2152 in FlnA, an event mediated by PKC- $\alpha$ . mTOR  
86 promoted recruitment of FlnA to sites of InlB-mediated entry. The GTPase RalA was  
87 also needed for FlnA recruitment. Depletion of FlnA by RNA interference (RNAi) or  
88 expression of a mutated form of FlnA that is not phosphorylated on serine 2152  
89 inhibited entry, indicating an important role for FlnA in infection by *Listeria*. Further  
90 experiments revealed that mTOR, PKC- $\alpha$ , and RalA each control exocytosis during

91 entry by recruiting the exocyst, a multicomponent complex known to promote  
92 exocytosis by tethering vesicles to sites in the plasma membrane (17). RNAi  
93 experiments demonstrated an important role for the exocyst complex in InlB-  
94 mediated entry. Collectively, these findings identify a host signaling pathway that  
95 controls the exocyst complex to promote infection of human cells by *Listeria*.

96

97

98

**RESULTS****99 The host scaffolding protein FlnA promotes InlB-mediated entry of *Listeria***

100 Previous results demonstrated that the host serine/threonine kinases mTOR and PKC-  
101  $\alpha$  act together to control InlB-mediated entry of *Listeria* (13). In order to better  
102 understand how these two kinases regulate InlB-dependent internalization, we  
103 focused our attention on FlnA, a protein that bundles actin filaments and assembles  
104 multi-molecular signaling complexes (18). This protein is known to interact with  
105 PKC- $\alpha$  or the mTORC2 component Rictor, and is directly phosphorylated by PKC- $\alpha$   
106 (19-22).

107 We used RNAi to examine the role of FlnA in InlB-mediated invasion of  
108 *Listeria* into the human epithelial cell line HeLa. In order to control for potential off-  
109 target effects (23), three different siRNAs targeting distinct sequences in FlnA mRNA  
110 were used. Control conditions included mock transfection in the absence of siRNA or  
111 transfection with a control “non-targeting” siRNA that lacks complementarity to any  
112 known mRNA. Importantly, each of the three siRNAs against FlnA reduced  
113 expression of the target protein and inhibited invasion of *Listeria* into HeLa cells  
114 compared to the control conditions (Fig. 1A,B).

115 We also determined the effect of siRNA-mediated depletion of FlnA on entry  
116 of inert particles coated with InlB. Latex beads (3  $\mu$ m in diameter) have been  
117 extensively used as a model for InlB-dependent entry, since these particles lack other  
118 bacterial factors and are efficiently internalized into mammalian cells in a manner that  
119 depends on the Met receptor and other host proteins involved in *Listeria* uptake (6,  
120 11-13, 24-28). As previously reported (6, 13, 26, 29), beads coupled to InlB were  
121 efficiently internalized into HeLa cells, whereas control beads coupled to glutathione  
122 S-transferase (GST), were not internalized (Fig. 1Ci). Next, the siRNA against FlnA

123 that caused the largest inhibition in invasion of *Listeria* was used to deplete FlnA in  
124 HeLa cells and the effect on uptake of InlB-coated beads was assessed. Internalization  
125 of beads was inhibited by about 40% (Fig. 1Cii). Taken together, the results in Figure  
126 1 indicate an important role for host FlnA in InlB-dependent entry.

127

### 128 **InlB induces PKC- $\alpha$ -dependent phosphorylation of FlnA**

129 FlnA is comprised of an amino-terminal actin binding domain and 24  
130 immunoglobulin (Ig)-like domains (18). One of the phosphorylation sites for FlnA is  
131 serine 2152, located in Ig domain 20. Phosphorylation of this residue controls several  
132 biological events, including focal adhesion formation, lamellipodia formation, protein  
133 trafficking, and cell migration (20, 22, 30-33).

134 We investigated whether the InlB-mediated pathway of entry involves  
135 phosphorylation of serine 2152 in FlnA. The effects of InlB on FlnA phosphorylation  
136 were assessed in two different conditions: treatment of mammalian cells with soluble  
137 InlB protein and entry of InlB-coated beads. When used at low nanomolar  
138 concentrations, soluble InlB is a potent agonist of the Met receptor and its associated  
139 downstream signaling pathways (3, 13, 34, 35). Importantly, treatment of HeLa cells  
140 with 4.5 nM of soluble InlB for 10 min caused an increase in reactivity of cell lysates  
141 with antibodies generated against phosphorylated serine 2152 in FlnA (Fig. 2Ai).  
142 Results from two types of control experiments indicated that these anti-phospho-FlnA  
143 antibodies recognize predominantly phosphorylated serine 2152 in FlnA in HeLa  
144 cells. First, transfection of HeLa cells with an siRNA targeting FlnA reduced  
145 reactivity with the anti-phospho-FlnA antibodies (Fig. 2Ai). Secondly, substitution of  
146 serine 2152 with an alanine residue (S2152A) decreased reactivity with these



147 antibodies (Fig. 2Aii). Collectively, the results in Figure 2A indicate that soluble InlB  
148 stimulates phosphorylation of serine 2152 in FlnA.

149         Several serine/threonine kinases including PAK1, p70S6K, and PKC- $\alpha$  are  
150 known to phosphorylate S2152 in FlnA (19 20, 30, 36). Since PKC- $\alpha$  plays an  
151 important role in InlB-mediated entry of *Listeria* (13), we examined if this kinase  
152 mediates phosphorylation of FlnA induced by InlB. Importantly, siRNA-mediated  
153 depletion of PKC- $\alpha$  reduced phosphorylation of FlnA on serine 2152 in HeLa cells  
154 treated with soluble InlB protein (Fig. 2B). The Met receptor is required for InlB-  
155 induced activation (phosphorylation) of PKC- $\alpha$  (13). As expected, siRNA-mediated  
156 knockdown of Met inhibited FlnA phosphorylation of serine 2152 (Fig. 2C). These  
157 results demonstrate that Met and PKC- $\alpha$  are needed for efficient phosphorylation of  
158 FlnA in response to InlB.

159         Experiments involving InlB-coated beads demonstrated that incubation with  
160 these particles stimulated phosphorylation of FlnA on serine 2152 (Figure 2D). These  
161 findings demonstrate that phosphorylation of FlnA increases during InlB-mediated  
162 entry.

163

#### 164 **Phosphorylation of FlnA contributes to InlB-mediated entry**

165 In order to determine if phosphorylation of FlnA on serine 2152 affects InlB-  
166 dependent internalization, we used a FlnA mutant protein containing a serine-to-  
167 alanine substitution at amino acid 2152. This S2152A mutation in FlnA causes defects  
168 in membrane ruffling (30), cell migration (32), or trafficking of the lipid raft  
169 component caveolin-1 (20), indicating that it perturbs FlnA function. We compared  
170 the efficiency of InlB-mediated entry into HeLa cells transiently expressing myc-  
171 tagged wild-type FlnA or FlnA.S2152A. The myc-FlnA wild-type and myc-

172 FlnA.S2152A proteins were expressed at similar levels, as assessed by Western  
173 blotting (Figure 3A) or confocal microscopy analysis (Fig. 3Bii). Importantly, entry  
174 of InlB-coated beads was about 35% lower into cells expressing myc-FlnA.S2152A  
175 compared to cells expressing the myc-FlnA wild-type protein (Fig. 3Bi). These results  
176 indicate that phosphorylation of FlnA on serine 2152 contributes to InlB-dependent  
177 uptake.

178

### 179 **mTOR and RalA mediate recruitment of FlnA during InlB-dependent entry**

180 Incubation of HeLa cells with InlB-coated beads resulted in accumulation of FlnA in  
181 cup-like structures around particles (Fig. 4A). By contrast, incubation with control  
182 GST-coated beads failed to induce FlnA accumulation. Accumulation of FlnA was  
183 quantified by measuring fold enrichment (FE) values, essentially as described (6, 13,  
184 28, 29). FE is defined as the mean fluorescence intensity of a host protein of interest  
185 in a cup-like structure around beads normalized to the mean fluorescence intensity of  
186 the protein throughout the entire human cell. An FE value greater than 1.0 indicates  
187 enrichment of the host protein around particles. The mean FE value for FlnA in  
188 control conditions involving HeLa cells that were mock transfected or transfected  
189 with control siRNA was about 1.35, indicating enrichment (Figure 4B). By  
190 comparison, the mean FE value for cells incubated with GST-coated beads was less  
191 than 1.0. These results demonstrate that InlB induces a redistribution of FlnA, causing  
192 this host protein to accumulate at sites of particle internalization.

193 We next examined the roles of mTOR, PKC- $\alpha$ , and Met in recruitment of  
194 FlnA during entry. We previously reported that siRNAs targeting mTOR, PKC- $\alpha$ , or  
195 Met inhibit entry of InlB-coated beads into HeLa cells (6, 13). Using these same

196 siRNAs, we found that RNAi against mTOR or Met, but not PKC- $\alpha$ , impaired  
197 accumulation of FlnA around InlB-coated beads (Figure 4).

198 FlnA is known to interact with the activated form of the GTPase RalA, and  
199 this interaction recruits FlnA to filopodia (37). We previously reported that RalA is  
200 needed for efficient entry of *Listeria* and InlB-coated beads into HeLa cells (6). Here  
201 we found that siRNA-mediated depletion of RalA prevented accumulation of FlnA  
202 around InlB-coated beads (Fig. 4). These results suggest that RalA may control InlB-  
203 dependent internalization, in part, through recruitment of FlnA. Taken together, the  
204 results in Figures 4 indicate that mTOR and RalA act upstream of FlnA to localize  
205 this protein to sites of InlB-mediated entry.

206

#### 207 **mTOR, PKC- $\alpha$ , and FlnA control exocytosis during InlB-mediated entry**

208 RNAi-based studies indicate that localized exocytosis during InlB-dependent entry  
209 requires the Met receptor and RalA (6). Since RalA controls recruitment of FlnA  
210 (Fig. 4), we tested the possibility that FlnA and its regulators mTOR and PKC- $\alpha$   
211 might promote exocytosis during InlB-mediated entry. Exocytosis was detected using  
212 a probe consisting of the v-SNARE protein VAMP3 fused to GFP (6, 38). Prior to  
213 exocytosis, VAMP3-GFP resides in intracellular vesicles. When vesicles fuse with the  
214 plasma membrane during exocytosis, the GFP moiety becomes extracellular  
215 (exofacial) and can be labeled with antibodies without cell permeabilization.

216 HeLa cells were subjected to control conditions or transfected with siRNAs  
217 against mTOR, PKC- $\alpha$ , FlnA, or Met. As a negative control for a condition  
218 previously found to not affect exocytosis, HeLa cells were transfected with an siRNA  
219 targeting the Arp3 component of the Arp2/3 complex (6, 29). After siRNA  
220 transfection, cells were transfected with a plasmid expressing VAMP3-GFP,

221 incubated with beads coated with InlB or GST, fixed, and labeled for exofacial  
222 VAMP3-GFP as described (6, 38). Images were acquired by confocal microscopy,  
223 and exocytosis was quantified as FE values for exofacial VAMP3-GFP, as described  
224 (6). The results indicate that siRNAs against mTOR, PKC- $\alpha$ , FlnA, or Met each  
225 reduced exocytosis around InlB-coated particles (Fig. 5). By contrast, the siRNA  
226 targeting Arp3 did not affect exocytosis around beads, consistent with previous  
227 findings (6). Importantly, experiments in this study or in previously published work  
228 indicate that each of the siRNAs used against mTOR, PKC- $\alpha$ , FlnA, Met, or Arp3  
229 inhibit target protein expression and internalization of InlB-coated beads (Fig. 1A,C)  
230 (6, 13, 26, 29). Taken together, the findings in Figure 5 demonstrate important  
231 functions for mTOR, PKC- $\alpha$ , and FlnA in exocytosis during InlB-dependent  
232 internalization.

233         Given the role of FlnA in exocytosis during entry, we next determined if  
234 phosphorylation of S2152 affects this host process. HeLa cells were co-transfected  
235 with plasmids expressing the exocytic probe VAMP3-GFP and myc-tagged wild-type  
236 FlnA or FlnA.S2152A. After acquisition of images using confocal microscopy, the  
237 degree of exocytosis in cells expressing either myc-tagged FlnA protein was  
238 quantified as FE values for exofacial VAMP3-GFP. The results, presented in Figure  
239 6, show that exocytosis was ~ 40% lower in cells expressing myc-FlnA.S2152A  
240 compared to in cells expressing wild-type FlnA. These findings indicate that  
241 phosphorylation of serine 2152 contributes to exocytosis during InlB-mediated entry.

242

243 **mTOR, PKC- $\alpha$ , RalA, and FlnA control exocytosis by recruiting the exocyst**  
244 **complex**

245 RalA is known to stimulate exocytosis through the exocyst complex (17, 39). This  
246 complex is comprised of eight proteins (Sec3, Sec5, Sec6, Sec8, Sec10, Sec15,  
247 Exo70, and Exo84) and tethers vesicles to the plasma membrane in a step preceding  
248 fusion of these vesicles with the plasma membrane. RNAi studies indicated roles for  
249 the exocyst components Sec3, Sec5, Sec8, and Exo70 in invasion of *Listeria* or entry  
250 of InlB-coated beads into HeLa cells (Figures 7 and S1).

251 Experiments with constructs comprised of Exo70, Sec5, Sec8, or Sec15 fused to  
252 GFP demonstrated that these host proteins accumulate around InlB-coated beads  
253 during particle entry (Fig. S2A). Immunolabeling of endogenous Exo70, Sec5, or  
254 Sec8 also indicated recruitment (Fig. S2B). Of all the endogenous or GFP-tagged  
255 proteins examined, GFP-Exo70 displayed the most pronounced accumulation around  
256 InlB-coated beads. We therefore assessed the roles of mTOR, PKC- $\alpha$ , RalA, and  
257 FlnA in GFP-Exo70 recruitment. Importantly, treatment of HeLa cells with siRNAs  
258 against mTOR, PKC- $\alpha$ , or FlnA each reduced accumulation of GFP-Exo70 around  
259 InlB-coated beads (Fig. 8). An siRNA targeting Arp3 did not affect accumulation of  
260 GFP-Exo70 around InlB-coated beads, consistent with the lack of effect of Arp3  
261 RNAi on exocytosis (Fig. 8) (6). Collectively, these results demonstrate that mTOR,  
262 PKC- $\alpha$ , RalA, and FlnA mobilize Exo70 to plasma membrane sites during particle  
263 internalization.

264 Further experiments demonstrated that the exocyst complex mediates exocytosis  
265 during InlB-dependent entry. RNAi-mediated depletion of Sec3, Sec5, Sec8, or  
266 Exo70 each reduced the accumulation of exofacial VAMP3-GFP that normally occurs  
267 around InlB-coated particles (Fig. 9). Taken together, the results in Figures 8 and 9  
268 demonstrate that mTOR, PKC- $\alpha$ , RalA, and FlnA control recruitment of the exocyst  
269 complex to promote exocytosis during InlB-dependent uptake.

270

**DISCUSSION**

271 In this study, we demonstrated that host mTOR, PKC- $\alpha$ , and FlnA each promote  
272 exocytosis during InlB-mediated entry of *Listeria*. Our previous results indicate that  
273 the host GTPase RalA also contributes to exocytosis during entry (6). The findings in  
274 this work, combined with the previous results with RalA, suggest that mTOR, PKC- $\alpha$ ,  
275 RalA, and FlnA form a signaling pathway that controls exocytosis through  
276 recruitment of Exo70, a component of the exocyst complex. Evidence for such a  
277 pathway is that PKC- $\alpha$  is needed for efficient phosphorylation of FlnA on serine  
278 2152, and that both mTOR and RalA mediate the recruitment of FlnA to sites of InlB-  
279 mediated uptake. Collectively, these results suggest that FlnA acts downstream of  
280 PKC- $\alpha$ , mTOR, and RalA during entry.

281 How do RalA and mTOR recruit FlnA the plasma membranes during InlB-  
282 dependent internalization? FlnA has 24 immunoglobulin (Ig)-like repeats that interact  
283 with at least 90 different binding partners, including various receptors, cytoskeletal  
284 proteins, transcription factors, and cytoplasmic signaling proteins (18). Importantly,  
285 activated RalA binds to Ig repeat 24 in FlnA, and this interaction recruits FlnA to  
286 filopodia (37). It is plausible that the same interaction is responsible for the ability of  
287 RalA to recruit FlnA during InlB-mediated uptake. In regard to mTOR, Ig repeat 21  
288 in FlnA is known to associate with Rictor (21, 22), an essential component of the  
289 mTOR-containing complex mTORC2 (16). mTORC2 has an important role in InlB-  
290 dependent internalization of *Listeria* (13). Future work should reveal whether  
291 mTORC2 contributes to recruitment of FlnA during InlB-mediated entry.

292 Our data indicate that phosphorylation of S2152 in FlnA participates in InlB-  
293 mediated uptake and exocytosis. Although phosphorylation of this site controls  
294 several biological processes including protein trafficking, cell adhesion, and cell

295 migration, how phosphorylation affects FlnA activity is not well understood (20, 22,  
296 30-33). There is some evidence to suggest that phosphorylation of serine 2152  
297 augments binding of ligands to Ig repeat 21 in FlnA (40). Serine 2152 is located in Ig  
298 repeat 20 of FlnA (18). Structural and computer modeling studies provide evidence  
299 that Ig repeat 20 controls the force-dependent interaction of ligands with Ig repeat 21  
300 in FlnA (18, 41). FlnA is an actin filament bundling protein that is subjected to  
301 mechanical forces exerted by actomyosin-mediated contractility (42). These forces  
302 lead to the displacement of a beta strand from Ig repeat 20 that would otherwise  
303 inhibit binding of ligands to Ig repeat 21 (42, 43). Interestingly, computer simulations  
304 predict that phosphorylation of serine 2152 lowers the force needed to relieve  
305 autoinhibition of binding to repeat 21 (40). Collectively, these structural, cell  
306 biological, and modeling studies suggest that phosphorylation of serine 2152A might  
307 enhance binding of ligands to Ig repeat 21 (40-43). This idea predicts that one or more  
308 ligands of Ig repeat 21 might participate in exocytosis during InlB-mediated entry.

309 Finally, our results indicate an important role for the host exocyst complex in  
310 entry of InlB-coated beads and in invasion of the wild-type *Listeria* strain EGD.  
311 Interestingly, strain EGD expresses higher levels of InlB than some other commonly  
312 studied strains of *Listeria* due the presence of an activated form of the transcription  
313 factor PrfA (44). In future work, it will be of interest to examine if FlnA and the  
314 exocyst complex play important roles in entry of *Listeria* strains apart from EGD.  
315 Like the *Listeria* strain EGD, the bacteria *Salmonella enterica* serovar typhimurium  
316 and *Staphylococcus aureus* exploit the exocyst complex in order to gain entry into  
317 human cells (45-47). An interesting question for future research is whether subversion  
318 of exocytosis through the exocyst is a general strategy used for internalization by  
319 bacterial pathogens.

320

**MATERIALS AND METHODS**321 *Bacterial strains, mammalian cell lines and media*

322 The *Listeria monocytogenes* strain BUG 947 was grown in brain heart infusion (BHI;  
323 Difco) broth and prepared for infection as described (34). This strain is derived from  
324 the wild-type strain EGD and contains an in-frame deletion in the *inlA* gene and is  
325 internalized into mammalian cells in a manner dependent on the *Listeria* protein InlB  
326 and its host receptor Met (3, 26, 48).

327 The human epithelial cell line HeLa (ATTC CCL-2) was grown in Dulbecco's  
328 modified Eagle's medium (DMEM) with 4.5 g of glucose per liter and 2 mM  
329 glutamine (catalog no. 11995-065; Life Technologies), supplemented with 5 or 10%  
330 fetal bovine serum (FBS). Cell growth, bacterial infections, incubations with latex  
331 beads, and stimulation with InlB protein were performed at 37°C under 5% CO<sub>2</sub>.

332

333 *Antibodies, inhibitors, and purified proteins*

334 Rabbit antibodies used were anti-InlB(3), anti-Met (4560; Cell Signaling  
335 Technology), anti-myc (PRB-150P; Covance), and anti-phospho-Filamin A (Serine  
336 2152) (Cell Signaling Technology; 4761). Mouse monoclonal antibodies used were,  
337 anti-Exo70 (ED2001; Kerafast), anti-Filamin A (Millipore; CBL228), anti-  
338 glutathione-S-transferase (GST) (G1160; Sigma-Aldrich), anti-GFP (11814460001;  
339 Sigma-Aldrich), anti-myc (9E10) (626802; Biolegend), normal mouse IgG (sc-2025;  
340 Santa Cruz Biotechnology), anti-Sec3 (HPA037706; Sigma-Aldrich); anti-Sec5  
341 (ED2002; Kerafast), anti-Sec8 (610658; Becton Dickenson) and anti-tubulin (T5168;  
342 Sigma-Aldrich). Horseradish peroxidase (HRPO)-conjugated secondary antibodies  
343 were purchased from Jackson Immunolabs. Secondary antibodies or phalloidin  
344 coupled to Alexa Fluor 488, Alexa Fluor 555, or Alexa Fluor 647 were obtained from



345 Life Technologies. 6XHis-tagged InlB or glutathione S-transferase proteins were  
346 expressed in *E. coli* and purified as previously described (34, 49). Okadaic acid and  
347 sodium orthovanadate were purchased from Sigma-Aldrich.

348

#### 349 *siRNAs*

350 The sequences of short interfering RNAs (siRNAs) used were 5'-  
351 GGAAUUGAGUGGUGGUAGAtt-3' (Arp3), 5'-  
352 GGUUAAAGGUGACUGAUUAAu-3' (Exo70-1), 5'-  
353 CAGACAACAUCAAGAAUGAtt-3' (Exo70-2), 5'-  
354 GACUGGCGUGUCAUUGGACAGAUAAAtt-3' (Exo70-3), 5'-  
355 CAGUCAAGUUCAACGAGGAtt-3' (FlnA #1), (2)  
356 GUGACCGCCAAUAACGACAuu (FlnA #2), 5'-CGAAGAAAGCCCGUGCCUAtt-  
357 3' (FlnA #3), 5'-CCAGAGACAUGUAUGAUAAu-3' (Met), 5'-  
358 GGAAAUGGGUUGAUGAACUtt-3' (mTOR), 5'-  
359 GCUCCACACUAAAUCCGCAAtt-3' (PKC- $\alpha$ ), 5'-  
360 CUGCAAUUAGAGACAACUAtt-3' (RalA), 5'-GAUUCAGUGAUUUGCGAGAtt-  
361 3' (Sec3-1), 5'-CACUAAACCUUGUGAAAGAtt-3' (Sec3-2), 5'-  
362 GAUUGCAUGGGCCCUUCGAtt-3' (Sec3-3), 5'-  
363 CUCAAUGUGCUUCAGCGAUtt-3' (Sec5-1), 5'-  
364 GUUAGCAUGGCCUCAUUGAtt-3' (Sec5-2), 5'-  
365 GUAAUUGCUGCUAUCUAGAtt-3' (Sec5-3), 5'-  
366 AGAACCUGCUUUCAUGCAAu-3' (Sec8-1), 5'-  
367 CUUGAUACCUCUCACUAUUt-3' (Sec8-2), and 5'-  
368 CCAGAAACAGUUAAGGCAAtt-3' (Sec8-3). These siRNAs were obtained from  
369 Sigma-Aldrich. The negative, non-targeting control siRNA molecule #1 (catalog no.

370 D-001210-01) was purchased from Dharmacon. This siRNA has two or more  
371 mismatches with all sequences in the human genome, indicating that it should not  
372 target host mRNAs.

373

#### 374 *Mammalian expression plasmids*

375 Mammalian expression vectors used were EGFP-C1 (Clontech), pcDNA-myc-FlnA.wt  
376 (Addgene # 8982; gift of John Blenis), pcDNA-myc-FlnA.S2152A (Addgene # 8983;  
377 gift of John Blenis), pEGFP-C3-Exo70 (Addgene #53761; gift of Channing Der), and  
378 VAMP3-GFP (38).

379

#### 380 *Transfection*

381 HeLa cells grown in 24 well plates or on 22- by 22-mm coverslips were transfected  
382 with siRNAs or plasmid DNA using lipofectamine 2000 (Life Technologies) as  
383 previously described (26, 50).

384

#### 385 *Coupling of proteins to latex beads*

386 InlB or GST proteins were coupled to carboxylate-modified latex beads 3  $\mu$ m in  
387 diameter (Polysciences; catalog no. 09850) using either passive binding or covalent  
388 linkage as described (6, 26).

389

#### 390 *Stimulation of mammalian cells with soluble InlB or beads coated with InlB*

391 HeLa cells were starved by incubation in DMEM without FBS for 9-10 h followed by  
392 addition of 300 ng/ml (4.5 nM) soluble InlB for 10 min at 37°C in 5%. In the case of  
393 experiments with beads, particles coated with InlB or GST were added at a ratio of  
394 approximately 5 beads per HeLa cell. Cells were centrifuged at 1000 rpm for 2 min to

395 enhance contact between beads and cells, and then incubated for 10 min at 37°C in  
396 5% CO<sub>2</sub>. After incubation with soluble InlB or beads, cells were then washed in cold  
397 PBS, and lysates were prepared for Western blotting or immunoprecipitation.

398

#### 399 *Western blotting and immunoprecipitation*

400 For experiments involving Western blotting of total cell lysates, HeLa cells were  
401 solubilized in radioimmunoprecipitation assay (RIPA) buffer (1% Triton X-100,  
402 0.25% sodium deoxycholate, 0.05% SDS, 50 mM Tris-HCl [pH 7.5], 2 mM EDTA,  
403 150 mM NaCl, 1 mM phenylmethylsulfonyl fluoride, and 10 mg/liter each of  
404 aprotinin and leupeptin. For experiments assessing phosphorylation of FlnA, cells  
405 were solubilized in RIPA buffer containing 3 mM sodium orthovanadate and 1 μM  
406 okadaic acid. Protein concentrations of lysates were determined using a bicinchoninic  
407 acid (BCA) assay kit (Pierce), and equal protein amounts of each sample were  
408 migrated on 7.5% SDS/polyacrylamide gels. For analysis of phosphorylation of myc-  
409 tagged FlnA proteins, cells were solubilized in lysis buffer containing 50 mM Tris-  
410 HCl pH 7.5, 150 mM NaCl, 1% Triton X-100, 2 mM EDTA, 1 mM PMSF, 1 μM  
411 okadaic acid, 1 mM vanadate, and 10 μg per ml each of aprotinin and leupeptin.  
412 Lysates were used to prepare immunoprecipitates with anti-FlnA antibody or normal  
413 mouse IgG as a control. Immunoprecipitations were performed using protein A/G  
414 agarose beads (Santa Cruz Biotechnology) as described (34). Immunoprecipitates  
415 were migrated on 7.5% SDS/polyacrylamide gels and Western blotted with anti-  
416 phospho-Filamin A (Serine 2152) antibodies. All Western blotting experiments  
417 involved transfer of samples to PVDF membranes, incubation with primary antibodies  
418 or secondary antibodies coupled to horse radish peroxidase, and detection using  
419 enhanced chemiluminescence (ECL) or ECL Plus reagents (GE Healthcare), as

420 described previously (3). Chemiluminescence was detected using an Odyssey imaging  
421 system (Li-Cor Biosciences). Bands in Western blot images were quantified using  
422 ImageJ software as described (51).

423

#### 424 *Bacterial invasion assays*

425 Invasion of *Listeria* was measured using gentamicin protection assays, as previously  
426 described (3, 29). HeLa cells were infected with *Listeria* approximately 48 h after  
427 transfection with siRNAs. Cells were infected for 1 h in the absence of gentamicin  
428 using a multiplicity of infection of 30:1, and then incubated in DMEM with 20  $\mu\text{g/ml}$   
429 gentamicin for an additional 2 h. Bacterial invasion efficiencies were first expressed  
430 as the percentage of the inoculum that survived gentamicin treatment. To obtain  
431 relative invasion values, absolute percent entry values in a given experiment were  
432 normalized to the value in cells subjected to mock transfection in the absence of  
433 siRNA.

434

#### 435 *Quantification of internalization of beads*

436 Beads coated with InlB or GST were added to HeLa cells growing on 22- by 22-mm  
437 coverslips. A ratio of approximately 5 particles to human cells was used. Cells were  
438 centrifuged at 1000 rpm for 2 min at room temperature and then incubated for 30 min  
439 at 37°C in 5% CO<sub>2</sub> to allow internalization of beads. Cells were then washed in PBS  
440 and fixed in PBS containing 3% paraformaldehyde (PFA). Samples were labeled with  
441 anti-InlB or anti-GST antibodies, using a previously described approach that  
442 distinguishes extracellular or intracellular particles (26). In the case of experiments  
443 involving myc-tagged FlnA proteins (Fig. 3A,B,C), samples were also labeled with  
444 mouse anti-myc antibodies to allow identification of transfected cells. Secondary

445 antibodies used for labeling were coupled to Alexa Fluor 488, Alexa Fluor 555, and  
446 Alexa Fluor 647. Labeled samples were mounted in Molviol with 1,4-  
447 diazabicyclo[2.2.2]octane (DABCO) as an anti-fade agent. Samples were analyzed for  
448 intracellular and extracellular beads using an Olympus BX51 epifluorescence  
449 microscope equipped with a 20x 0.75 NA dry objective lens and an Olympus DP80  
450 CCD camera, using Olympus cellSens software (version 1.13). The data shown in  
451 Figures 1C, 3B, and S1 are from three experiments. In each experiment, at least 100  
452 intracellular beads were scored for the control conditions involving mock transfection  
453 in the absence of siRNA. A similar number of total (intracellular plus extracellular)  
454 beads were analyzed for all other conditions. Data were initially expressed as the  
455 percentage of total cell-associated beads that were internalized. These data were then  
456 converted to relative internalization values by normalizing to percent internalization  
457 data from controls lacking siRNA.

458

#### 459 *Confocal microscopy analysis*

460 For studies involving exocytosis in Figures 5 and 9, HeLa cells grown on 22- x 22-  
461 mm coverslips were transfected with siRNAs and then transfected again 24 h later  
462 with a plasmid expressing VAMP3 fused to GFP (VAMP3-GFP). Approximately 24  
463 h after addition of plasmid DNA, cells were washed, placed in serum-free DMEM,  
464 and incubated for 5 min in serum-free DMEM with InlB- or GST-coated beads, as  
465 described above. HeLa cells were washed in PBS and incubated with mouse anti-GFP  
466 antibodies for 1 h at 4°C. Cells were then fixed in PBS with 3% PFA, and incubated  
467 with anti-mouse antibodies coupled to Alexa Fluor 647 for 1 h. This method resulted  
468 in labeling of exofacial VAMP3-GFP (6, 38). Extracellular beads were labeled by  
469 incubation with anti-InlB or anti-GST antibodies, followed by secondary antibodies

470 conjugated to Alexa Fluor 555. Experiments to determine effect of myc-tagged FlnA  
471 proteins on exocytosis (Fig. 6) were performed similarly to the exocytosis studies  
472 described above, except that HeLa cells were co-transfected with plasmids expressing  
473 VAMP3-GFP and either myc-FlnA.wt or myc-FlnA-S2152A. After exofacial labeling  
474 of VAMP3-GFP with mouse anti-GFP antibodies, cells were permeabilized in PBS  
475 containing 0.4% Triton X-100, and myc-tagged proteins were labeled with rabbit anti-  
476 myc antibodies and anti-rabbit-Alexa Fluor 555. Experiments assessing recruitment of  
477 GFP-Exo70 (Fig. 8) were performed similarly to the exocytosis experiments, except  
478 that the exofacial labelling step with anti-GFP antibodies was omitted. For labeling of  
479 endogenous Exo70, Sec5, or Sec8 (Fig. S2B), cells were fixed by incubation in  
480 methanol for 5 min at -20°C. Samples were then incubated overnight at 4°C with  
481 primary antibodies in PBS with 1.0% BSA and 0.1% Tween 20.

482 All samples analyzed by confocal microscopy were mounted in Molviol  
483 supplemented with DABCO. Imaging was performed with an inverted Olympus  
484 FV1200 laser scanning confocal microscope, using a 60x 1.35 NA oil immersion  
485 objective, laser lines of 488 nm, 543 nm, and 633 nm, and photomultiplier tubes for  
486 detection. Images from serial sections spaced 1.0  $\mu\text{m}$  apart were used to ensure that  
487 all cell-associated beads were detected. Image J (version 1.51e) software was  
488 employed to determine fold enrichment (FE) values for each cell-associated bead. FE  
489 is defined as the mean pixel intensity in a ring-like structure around the bead,  
490 normalized to the mean pixel intensity throughout the human cell (6, 13, 28, 29). The  
491 thresholding function of Image J was used to measure mean pixel intensities in ring-  
492 like structures of FlnA, exofacial VAMP3-GFP, or GFP-Exo70 around beads. This  
493 function was also used to measure mean pixel intensity throughout the cell. In each  
494 experiment, approximately 50-100 extracellular, cell-associated beads were analyzed

495 for each condition. The data shown in Figures 4B, 5B, 6B, 8B, and 9B are pooled FE  
496 values from three or four independent experiments.

497

498 *Statistical analysis*

499 Statistical analysis was performed using Prism (version 6.0c; GraphPad Software). In  
500 comparisons of data from three or more conditions, analysis of variance (ANOVA)  
501 was used. The Tukey-Kramer test was used as a posttest. For comparisons of two data  
502 sets, Student's t-test was used. A P-value of 0.05 or lower was considered significant.

503

504

**ACKNOWLEDGEMENTS**

505 We thank Segolene de Champs for initial imaging studies with GFP-tagged exocyst  
506 proteins. This work was supported by grants from the Marsden Fund of the Royal  
507 Society of New Zealand (13-UOO-085), the Health Research Council of New  
508 Zealand (17/082), the University of Otago Research Committee, and the Dean's  
509 Bequest Fund (Otago School of Biomedical Sciences, University of Otago), awarded  
510 to K. Ireton.

511

512

513



514

**FIGURE LEGENDS**

515 **Figure 1. Host FlnA promotes InlB-mediated entry.** HeLa cells were either mock  
516 transfected in the absence of siRNA, transfected with a control non-targeting siRNA,  
517 or transfected with three different siRNAs against FlnA. About 48 h after transfection,  
518 cell lysates were prepared for analysis of target gene expression by Western blotting,  
519 or cells were incubated with *Listeria* or InlB-coated beads for assessment of invasion  
520 or entry, respectively. A. Effect of siRNAs against FlnA on target protein expression.  
521 A representative blot showing depletion of FlnA is displayed. After reaction with anti-  
522 FlnA antibodies, the membrane was stripped and probed with anti-tubulin antibodies  
523 to confirm equivalent loading. The adjacent bar graph displays mean +/- SEM values  
524 of quantified Western blotting data from three independent experiments. B. Effect of  
525 siRNAs targeting FlnA on invasion of *Listeria* expressing InlB. Results are mean +/-  
526 SEM relative entry values from three to six independent gentamicin protection  
527 experiments, depending on the condition. C. Effect of an siRNA targeting FlnA on  
528 entry of InlB-coated beads. (i). Internalization of beads coated with InlB or GST into  
529 HeLa cells. Data are the mean percentage of total cell-associated beads internalized  
530 +/- SEM from three independent experiments. 'ND' indicates that no internalized  
531 beads were detected. (ii). Decreased entry of InlB-coated beads into HeLa cells  
532 transfected with FlnA siRNA. The siRNA against FlnA used was #2. Results are  
533 mean relative entry values +/- SEM from three independent experiments. \*, P < 0.05  
534 compared to the control siRNA condition, as determined by ANOVA and the Tukey-  
535 Kramer posttest.

536

537 **Figure 2. InlB stimulates PKC- $\alpha$  -dependent phosphorylation of FlnA.** A.  
538 Specificity of anti-phospho-FlnA antibodies. (i). Effect of FlnA RNAi on reactivity

539 with antibodies. HeLa cells were either transfected with a control siRNA or with an  
540 siRNA targeting FlnA. Cell lysates were prepared and used for Western blotting with  
541 antibodies that recognize phosphorylated serine 2152 in FlnA. The left panel shows a  
542 representative Western blot and the right panel displays quantified Western blotting  
543 data as mean  $\pm$  SEM values from three independent experiments. (ii). Effect of  
544 mutation of serine 2152 on antibody reactivity. HeLa cells were transfected with  
545 plasmids expressing myc-tagged wild-type (wt) FlnA or FlnA containing a serine-to-  
546 alanine substitution in residue 2152 (S2152A). After transfection, lysates were  
547 prepared and used for immunoprecipitation with anti-myc antibodies or mock  
548 precipitation with control IgG. Precipitates were Western blotted using anti-phospho-  
549 FlnA (serine 2152) antibodies. Shown is a representative Western blot from one of  
550 two experiments performed. (B). Effect of depletion of PKC- $\alpha$  on phosphorylation of  
551 FlnA. After transfection of HeLa cells with control siRNA or an siRNA against PKC-  
552  $\alpha$ , lysates were prepared and used for Western blotting with antibodies against  
553 phosphorylated serine 2152 in FlnA, total FlnA, PKC- $\alpha$ , or tubulin. (i).  
554 Representative Western blots are shown. (ii). Quantified Western blotting data  
555 expressed as mean  $\pm$  SEM values from six independent experiments are presented.  
556 (C). Effect of depletion of Met on phosphorylation of FlnA. (i). Representative  
557 Western blotting results are shown. (ii). Quantified Western blotting data expressed as  
558 mean  $\pm$  SEM values from seven independent experiments are displayed. (D).  
559 Phosphorylation of FlnA during InlB-mediated entry. HeLa cells were incubated with  
560 latex beads coupled to InlB or GST for 10 min, followed by solubilization in lysis  
561 buffer. Lysates were Western blotted with anti-phospho-FlnA (serine 2152)  
562 antibodies. (i). A representative Western blot is shown. (ii). Quantified Western

563 blotting data expressed as mean +/- SEM values from three independent experiments  
564 are presented. \*,  $P < 0.05$ , as determined by ANOVA and the Tukey-Kramer posttest.

565

566 **Figure 3. Phosphorylation of FlnA on serine 2152 contributes to InlB-mediated**

567 **entry.** HeLa cells were transfected with plasmids expressing myc-tagged wild-type

568 (WT) FlnA or FlnA containing a serine-to-alanine substitution in residue 2152

569 (S2152A). About 24 h after transfection, lysates were prepared for evaluation of

570 tagged FlnA protein expression by Western blotting or fixed samples were made for

571 fluorescence microscopy analysis of entry of InlB-coated beads. A. Expression of

572 myc-tagged FlnA proteins assessed by Western blotting. The panel on the left shows a

573 representative Western blot, whereas the graph on the right displays quantified

574 Western blotting data as mean +/-SEM values from three independent experiments. B.

575 Entry of InlB-coated beads. (i). The percentage of cell-associated beads that were

576 internalized into HeLa cells expressing myc-tagged FlnA.WT or FlnA.S2152A

577 proteins is shown. (ii). Expression of myc-tagged FlnA proteins in the same samples

578 used for analysis of internalization of InlB-coated beads. Pixel intensities in HeLa

579 cells associated with InlB-coated beads were quantified using Image J software. The

580 data in (i) and (ii) are mean +/- SEM values from four independent experiments. \*,  $P$ ,

581  $< 0.05$ , as determined by Student's t-test.

582

583 **Figure 4. FlnA is recruited during entry in a manner that depends on mTOR, RalA,**

584 **and Met.** HeLa cells were mock transfected in the absence of siRNA, transfected with

585 a control siRNA, or transfected with siRNAs targeting mTOR, PKC- $\alpha$ , RalA, or Met.

586 Cells were then incubated for 10 min with beads coupled to InlB or to GST, followed

587 by fixation and labeling for confocal microscopy. A. Confocal microscopy images of

588 localization of endogenous FlnA. Panels on the left show FlnA localization in HeLa  
589 cells, with locations of beads indicated with arrows. Regions near beads are expanded  
590 in the middle and right panels. Middle panels show FlnA labeling, whereas right  
591 panels are differential interference contrast (DIC) images displaying beads. Scale bars  
592 indicate 5 micrometers. B. Quantification of recruitment of FlnA. Data are pooled  
593 fold enrichment (FE) values from four independent experiments. Each dot represents  
594 a single FE value. Horizontal bars are means and error bars are SD. \*,  $P < 0.05$   
595 compared to the no siRNA and control siRNA conditions.

596

597 **Figure 5. *mTOR*, *PKC- $\alpha$* , and *FlnA* control exocytosis during *InlB*-mediated entry.**

598 HeLa cells were mock transfected in the absence of siRNA, transfected with a control  
599 siRNA, or transfected with siRNAs targeting mTOR, PKC- $\alpha$ , FlnA, Met, or Arp3.  
600 Cells were then transfected with a plasmid expressing the exocytic probe VAMP3-  
601 GFP and incubated for 5 min with beads coupled to InlB or to GST. Samples were  
602 fixed and labeled for confocal microscopy. A. Representative confocal microscopy  
603 images. Total VAMP3-GFP is green, exofacial VAMP3-GFP is red, and beads are  
604 blue. Panels on the left are merged images of single HeLa cells, with locations of  
605 beads indicated with arrows. Regions near beads are expanded in panels to the right.  
606 Scale bars indicate 5 micrometers. B. Quantification of exocytosis. Data are pooled  
607 FE values of exofacial VAMP3-GFP from three to four independent experiments,  
608 depending on the condition. Dots represent individual FE values. Horizontal bars are  
609 means and error bars are SD. \*,  $P < 0.05$  compared to the control siRNA condition, as  
610 determined by ANOVA and the Tukey-Kramer posttest.

611

612 **Figure 6. Phosphorylation of serine 2152 in *FlnA* contribute to exocytosis.**

613 HeLa cells were co-transfected with plasmids expressing VAMP3-GFP and either  
614 myc-tagged wild-type (wt) FlnA or FlnA.S2152A. Cells were then incubated with  
615 InlB-coated beads for 5 min, followed by labeling for exofacial VAMP3-GFP and  
616 myc-tagged proteins. Confocal microscopy was performed to acquire images for  
617 quantification of exocytosis. A. Representative microscopy images. Myc-tagged FlnA  
618 proteins are colored blue, VAMP3-GFP is green, exofacial VAMP3-GFP is red, and  
619 beads are detected using differential interference contrast (DIC) microscopy. Panels  
620 on the left are merged images of single HeLa cells, with locations of beads indicated  
621 with arrows. Regions near beads are expanded in panels to the right. Scale bars  
622 indicate 5 micrometers. B. (i). Quantification of exocytosis. Data are pooled FE  
623 values of exofacial VAMP3-GFP from three independent experiments. Dots represent  
624 individual FE values. Horizontal bars are means and error bars are SD. (ii).  
625 Expression of myc-tagged FlnA proteins in the same samples used for analysis of  
626 exocytosis. Pixel intensities in HeLa cells associated with InlB-coated beads were  
627 quantified using Image J software. The data are mean pixel intensities +/- SEM from  
628 three independent experiments. \*,  $P < 0.05$ , as determined by Student's t-test.

629

630 **Figure 7. The exocyst complex promotes InlB-dependent invasion of *Listeria*.** HeLa  
631 cells were mock transfected in the absence of siRNA, transfected with a control  
632 siRNA, or transfected with siRNAs against the exocyst components Sec3, Sec5, Sec8,  
633 or Exo70. About 48 h after transfection, cells were solubilized for assessment of  
634 target protein expression or infected with wild-type *Listeria* for analysis of invasion.  
635 A. Effect of siRNAs on Sec3 expression and invasion of *Listeria*. (i). Sec3 expression.  
636 The left panel shows a representative Western blot indicating depletion of Sec3 by  
637 siRNAs. The right panel is quantified Western blotting data showing mean relative

638 Sec3 expression +/- SEM from three independent experiments. (ii). Invasion of  
639 *Listeria*. Data are mean relative entry values +/- SEM from three to eight independent  
640 experiments, depending on the siRNA. B. siRNA-mediated inhibition in Sec5  
641 expression and invasion of *Listeria*. (i). Sec5 expression. In the left panel, a  
642 representative Western blot is shown. The right panel displays quantified Western  
643 blotting data from three independent experiments. (ii). Invasion of *Listeria*. Data are  
644 means +/- SEM from three to six independent experiments. C. Reduction in  
645 expression of Sec8 and invasion of *Listeria* by siRNAs. (i). Sec8 expression. (i). In  
646 the left panel, a representative Western blot is presented. The right panel shows  
647 quantified Western blotting data from three independent experiments. (ii). Invasion of  
648 *Listeria*. Data are means +/- SEM of three to six independent experiments. D. siRNA-  
649 mediated inhibition in expression of Exo70 and invasion of *Listeria*. (i). Exo70  
650 expression. The left panel shows a representative Western blot and the right panel  
651 displays quantitative Western blotting data from three independent experiments. (ii).  
652 Invasion of *Listeria*. Data are means +/- SEM from three independent experiments. \*,  
653  $P < 0.05$ , as determined by ANOVA and the Tukey-Kramer posttest.

654

655 **Figure 8. *mTOR*, *PKC- $\alpha$* , *RalA*, and *FlnA* mediate recruitment of *Exo70* during**  
656 ***InlB*-mediated entry.** HeLa cells were subjected to control conditions or transfected  
657 with siRNAs against mTOR, PKC- $\alpha$ , RalA, FlnA, Met, or Arp3. Cells were then  
658 transfected with a plasmid expressing Exo70 fused to GFP (GFP-Exo70). After  
659 transfection, cells were incubated for 5 min with beads coupled to InlB or to GST,  
660 followed by fixation and labeling for confocal microscopy. A. Representative  
661 confocal microscopy images. GFP-Exo70 is green and beads are red. Panels on the  
662 left are merged images of single HeLa cells. Arrows indicate beads. Regions near

663 beads are expanded in the panels to the right. Scale bars indicate 5 micrometers. B.  
664 Quantification of recruitment of GFP-Exo70. Data are pooled FE values of GFP-  
665 Exo70 from three independent experiments. Dots represent individual FE values.  
666 Horizontal bars are means and error bars are SD. \*,  $P < 0.05$  compared to the control  
667 siRNA condition, as assessed by ANOVA and the Tukey-Kramer posttest.

668

669 **Figure 9. *The exocyst complex promotes exocytosis during InlB-mediated entry.***

670 HeLa cells were subjected to control conditions or transfected with siRNAs against  
671 Sec3, Sec5, Sec8, or Exo70. Cells were then transfected with a plasmid expressing  
672 VAMP3-GFP. After transfection, cells were incubated for 5 min with beads coupled  
673 to InlB, followed by fixation and labeling for confocal microscopy. Scale bars  
674 indicate 5 micrometers. A. Representative confocal microscopy images. Total  
675 VAMP3-GFP is green, exofacial VAMP3-GFP is red, and beads are blue. Panels on  
676 the left are merged images of single HeLa cells, with beads being indicated by arrows.  
677 Regions near beads are expanded in panels to the right. B. Quantification of  
678 exocytosis. Data are pooled FE values of exofacial VAMP3-GFP from three  
679 independent experiments. Dots represent individual FE values. Horizontal bars are  
680 means and error bars are SD. \*,  $P < 0.05$  compared to the no siRNA or control  
681 siRNA conditions, as determined by ANOVA and the Tukey-Kramer posttest.

682

683

684

685  
686

## REFERENCES

- 687 1. Posfay-Barbe KM, Wald ER. 2009. Listeriosis. *Semin Fetal Neonatal Med*  
688 14:228-233. <https://doi.org/10.1016/j.siny.2009.01.006>.
- 689 2. Disson O, Lecuit M. 2013. *In vitro* and *in vivo* models to study human  
690 listeriosis: mind the gap. *Microbes Infect* 15:971-980.  
691 <https://doi.org/10.1016/j.micinf.2013.09.012>.
- 692 3. Shen Y, Naujokas M, Park M, Ireton K. 2000. InlB-dependent internalization  
693 of *Listeria* is mediated by the Met receptor tyrosine kinase. *Cell* 103:501-510.  
694 [https://doi.org/10.1016/S0092-8674\(00\)00141-0](https://doi.org/10.1016/S0092-8674(00)00141-0).
- 695 4. Pizarro-Cerda J, Kühbacher A, Cossart P. 2012. Entry of *Listeria*  
696 monocytogenes in mammalian epithelial cells: an updated view. *Cold Spring*  
697 *Harb Perspect Med* 2:a010009. <https://doi.org/10.1101/cshperspect.a010009>.
- 698 5. Kuhbacher A, Emmenlauer M, Ramo P, Kafai N, Dehio C, Cossart P, Pizarro-  
699 Cerda J. 2015. Genome-wide siRNA screen identifies complementary  
700 signaling pathways involved in *Listeria* infection and reveals different actin  
701 nucleation mechanisms during *Listeria* cell invasion and actin comet tail  
702 formation. *mBio* 6:e00598-00515. <https://doi.org/10.1128/mBio.00598-15>.
- 703 6. Van Ngo H, Bhalla M, Chen DY, Ireton K. 2017. A role for host exocytosis in  
704 InlB-mediated entry of *Listeria monocytogenes*. *Cell Microbiol* 19:e12768.  
705 <https://doi.org/10.1111/cmi.12768>.
- 706 7. Ireton K, Rigano LA, Dowd GC. 2014. Role of host GTPases in infection by  
707 *Listeria monocytogenes*. *Cell Microbiol* 16:1311-1320. <https://doi.org/10.1111/cmi.12324>.
- 708  
709 8. Hong WJ, Lev S. 2014. Tethering the assembly of SNARE complexes. *Trends*  
710 *Cell Biol* 24:35-43. <https://doi.org/10.1016/j.tcb.2013.09.006>.



- 711 9. Daumke O, Roux A, Haucke V. 2014. BAR domain scaffolds in Dynamin-  
712 mediated membrane fission. *Cell* 156:882-892. [https://doi.org/](https://doi.org/10.1016/j.cell.2014.02.017)  
713 [10.1016/j.cell.2014.02.017](https://doi.org/10.1016/j.cell.2014.02.017).
- 714 10. Veiga E, Cossart P. 2005. Listeria hijacks the clathrin-dependent endocytic  
715 machinery to invade mammalian cells. *Nat Cell Biol* 7:894-900.  
716 <https://doi.org/10.1038/ncb1292>.
- 717 11. Bierne H, Gouin E, Roux P, Caroni P, Yin HL, Cossart P. 2001. A role for  
718 cofilin and LIM kinase in Listeria-induced phagocytosis. *Journal of Cell*  
719 *Biology* 155:101-112. <https://doi.org/10.1083/jcb.200104037>.
- 720 12. Bierne H, Miki H, Innocenti M, Scita G, Gertler FB, Takenawa T, Cossart P.  
721 2005. WASP-related proteins, Abi and Ena/VASP are required for Listeria  
722 invasion induced by the Met receptor. *J Cell Sci* 118:1537-1547. .  
723 <https://doi.org/10.1242/jcs.02285>.
- 724 13. Bhalla M, Law D, Dowd GC, Ireton K. 2017. Host serine-threonine kinases  
725 mTOR and Protein Kinase C- $\alpha$  promote InlB-mediated entry of Listeria  
726 monocytogenes. *Infect Immun* 85:pil: e00087-00017.  
727 <https://doi.org/10.1128/IAI.00087-17>.
- 728 14. Bracho-Valdes I, Moreno-Alvarez P, Valencia-Martinez I, Robles-Molina E,  
729 Chavez-Vargas L, Vazquez-Prado J. 2011. mTORC1- and mTORC2-  
730 interacting proteins keep their multifunctional partners focused. *IUBMB Life*  
731 63:896-914. <https://doi.org/10.1002/iub.558>.
- 732 15. Morrison MM, Young CD, Wang S, Sobolik T, Sanchez VM, Hicks DJ, Cook  
733 RS, Brantley-Sieders DM. 2015. mTOR directs breast morphogenesis through  
734 the PKC- $\alpha$ -Rac1 Signaling Axis. *PLoS Genet* 11:e1005291.  
735 <https://doi.org/10.1371/journal.pgen.1005291>.

- 736 16. Gaubitz C, Prouteau M, Kusmider B, Loewith R. 2016. TORC2 Structure and  
737 Function. *Trends Biochem Sci* 41:532-545. [https://doi.org/](https://doi.org/10.1016/j.tibs.2016.04.001)  
738 10.1016/j.tibs.2016.04.001.
- 739 17. Wu B, Guo W. 2015. The exocyst at a glance. *J Cell Sci* 128 2957-2964.  
740 [https://doi.org/doi: 10.1242/jcs.156398](https://doi.org/doi:10.1242/jcs.156398).
- 741 18. Razinia Z, Makela T, Ylanne J, Calderwood DA. 2012. Filamins in  
742 mechanosensing and signaling. *Annu Rev Biophys* 41:227-246.  
743 <https://doi.org/10.1146/annurev-biophys-050511-102252>.
- 744 19. Tigges U, Koch B, Wissing J, Jockush BM, Ziegler WH. 2003. The F-actin  
745 cross-linking and focal adhesion protein filamin A is a ligand and in vivo  
746 substrate for protein kinase C alpha. *J Biol Chem* 278:23561-23569.  
747 <https://doi.org/10.1074/jbc.M302302200>.
- 748 20. Muriel O, Echarri A, Hellriegel C, Pavon DM, Beccari L, Del Pozo MA.  
749 2011. Phosphorylated filamin A regulates actin-linked caveolae dynamics. *J*  
750 *Cell Sci* 124:2763-2776. <https://doi.org/10.1242/jcs.080804>.
- 751 21. Chantaravisoot N, Wongkongkathep P, Loo JA, Mischel PS, Tamanoi F.  
752 2015. Significance of filamin A in mTORC2 function in glioblastoma. *Mol*  
753 *Cancer* 14:127. [https://doi.org/doi: 10.1186/s12943-015-0396-z](https://doi.org/doi:10.1186/s12943-015-0396-z).
- 754 22. Sato T, Ishii J, Ota Y, Sasaki E, Shibagaki Y, Hattori S. 2016. Mammalian  
755 target of rapamycin (mTOR) complex 2 regulates filamin A-dependent focal  
756 adhesion dynamics and cell migration. *Genes Cells* 21:579-593.  
757 <https://doi.org/10.1111/gtc.12366>.
- 758 23. Mohr SE, Smith JA, Shamu CE, Neumuller RA, Perrimon N. 2014. RNAi  
759 screening comes of age: improved techniques and complementary approaches.  
760 *Nat Rev Mol Cell Biol* 15:591-600. [https://doi.org/ 10.1038/nrm3860](https://doi.org/10.1038/nrm3860).

- 761 24. Braun L, Ohayon H, Cossart P. 1998. The InIB protein of *Listeria*  
762 *monocytogenes* is sufficient to promote entry into mammalian cells.  
763 *Molecular Microbiology* 27:1077-1087. [https://doi.org/10.1046/j.1365-](https://doi.org/10.1046/j.1365-2958.1998.00750.x)  
764 [2958.1998.00750.x](https://doi.org/10.1046/j.1365-2958.1998.00750.x)
- 765 25. Seveau S, Bierne H, Giroux S, Prevost MC, Cossart P. 2004. Role of lipid  
766 rafts in E-cadherin- and HGF-R/Met-mediated entry of *Listeria*  
767 *monocytogenes* into host cells. *J Cell Biol* 166:743-753.  
768 <https://doi.org/10.1083/jcb.200406078>.
- 769 26. Dokainish H, Gavicherla B, Shen Y, Ireton K. 2007. The carboxyl-terminal  
770 SH3 domain of the mammalian adaptor CrkII promotes internalization of  
771 *Listeria monocytogenes* through activation of host phosphoinositide 3-kinase.  
772 *Cell Microbiol* 10:2497-2516. [https://doi.org/10.1111/j.1462-](https://doi.org/10.1111/j.1462-5822.2007.00976.x)  
773 [5822.2007.00976.x](https://doi.org/10.1111/j.1462-5822.2007.00976.x).
- 774 27. Veiga E, Guttman JA, Bonazzi M, Boucrot E, Toledo-Arana A, Lin Ae,  
775 Enninga J, Pizarro-Cerda J, Finlay BB, Kirchhausen T, Cossart P. 2007.  
776 Invasive and adherent bacterial pathogens co-opt host clathrin for infection.  
777 *Cell Host Microbe* 2:340-351. <https://doi.org/10.1016/j.chom.2007.10.001>.
- 778 28. Gavicherla B, Ritchey L, Gianfelice A, Kolokoltsov AA, Davey RA, Ireton K.  
779 2010. Critical role for the host GTPase-activating protein ARAP2 in InIB-  
780 mediated entry of *Listeria monocytogenes*. *Infect Immun* 78:4532-4541.  
781 <https://doi.org/doi:10.1128/IAI.00802-10>.
- 782 29. Dowd GC, Bhalla M, Kean B, Thomas R, Ireton K. 2016. Role of host type IA  
783 Phosphoinositide 3-kinase pathway components in invasin-mediated  
784 internalization of *Yersinia enterocolitica*. *Infect Immun* 84:1826-1841.  
785 <https://doi.org/10.1128/IAI.00142-16>.

- 786 30. Vadlamudi RK, Li F, Adam L, Nguyen D, Ohta Y, Stossel TP, Kumar R.  
787 2002. Filamin is essential in actin cytoskeletal assembly mediated by p21-  
788 activated kinase 1. *Nat Cell Biol* 4:681-690. <https://doi.org/10.1038/ncb838>.
- 789 31. Maceyka M, Alvarez SE, Milstien S, Spiegel S. 2008. Filamin A links  
790 sphingosine kinase 1 and sphingosine-1-phosphate receptor 1 at lamellipodia  
791 to orchestrate cell migration. *Mol Cell Biol* 28:5687-5697.  
792 <https://doi.org/doi:10.1128/MCB.00465-08>.
- 793 32. Li L, Lu Y, Stemmer PM, Chen F. 2015. Filamin A phosphorylation by Akt  
794 promotes cell migration in response to arsenic. *Oncotarget* 6:12009-12019.  
795 <https://doi.org/10.18632/oncotarget.3617>.
- 796 33. Pons M, Izquierdo I, Andreu-Carbo M, Garrido G, Planaguma J, Muriel O,  
797 Del Pozo MA, Geli MI, Aragay AM. 2017. Phosphorylation of filamin A  
798 regulates chemokine receptor CCR2 recycling. *J Cell Sci* 130:490-501.  
799 <https://doi.org/10.1242/jcs.193821>.
- 800 34. Ireton K, Payrastra B, Cossart P. 1999. The *Listeria monocytogenes* protein  
801 InlB is an agonist of mammalian phosphoinositide-3-kinase. *J Biol Chem*  
802 274:17025-17032. <https://doi.org/10.1074/jbc.274.24.17025>.
- 803 35. Sun H, Shen Y, Dokainish H, Holgado-Madruga M, Wong A, Ireton K. 2005.  
804 Host adaptor proteins Gab1 and CrkII promote InlB-dependent entry of  
805 *Listeria monocytogenes*. *Cell Microbiol* 7:443-457.  
806 <https://doi.org/10.1111/j.1462-5822.2004.00475.x>.
- 807 36. Woo MS, Ohta Y, Rabinovitz I, Stossel TP, Blenis J. 2004. Ribosomal S6  
808 kinase (RSK) regulates phosphorylation of filamin A on an important  
809 regulatory site. *Mol Cell Biol* 24:3025-3035.  
810 <https://doi.org/10.1128/MCB.24.7.3025-3035.2004>.

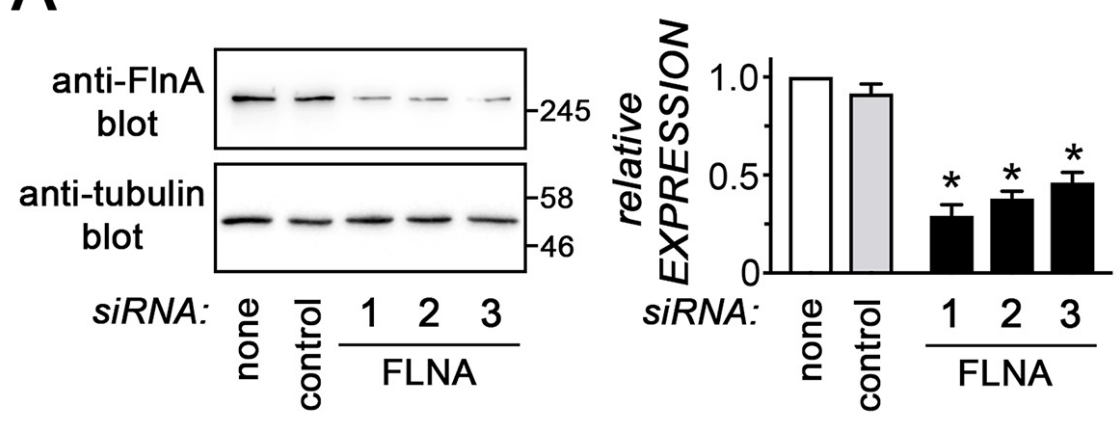
- 811 37. Ohta Y, Suzuki N, Nakamura S, Hartwig JH, Stossel TP. 1999. The small  
812 GTPase RalA targets filamin to induce filopodia. *Proc Natl Acad Sci USA*  
813 96:2122-2128. <https://doi.org/10.1073/pnas.96.5.2122>.
- 814 38. Bajno L, Peng XR, Schrieber AD, Moore HP, Trimble WS, Grinstein S. 2000.  
815 Focal exocytosis of VAMP3-containing vesicles at sites of phagosome  
816 formation. *J Cell Biol* 149:697-705. <https://doi.org/10.1083/jcb.149.3.697>.
- 817 39. Gentry LR, Martin TD, Reiner DJ, Der CJ. 2014. Ral small GTPase signaling  
818 and oncogenesis: More than just 15 minutes of fame. *Biochim Biophys Acta*  
819 1843:2976-2988. <https://doi.org/10.1016/j.bbamcr.2014.09.004>.
- 820 40. Chen HS, Kolahi KS, Mofrad MRK. 2009. Phosphorylation facilitates the  
821 integrin binding of filamin under force. *Biophys J* 97:3095-3104.  
822 <https://doi.org/10.1016/j.bpj.2009.08.059>.
- 823 41. Lad Y, Kiema T, Jiang P, Pentikainen OT, Coles CH, Campbell ID,  
824 Calderwood DA, Ylanne J. 2007. Structure of three tandem filamin domains  
825 reveals auto-inhibition of ligand binding. *EMBO J* 26:3993-4004.  
826 <https://doi.org/10.1038/sj.emboj.7601827>.
- 827 42. Nakamura F, Song M, Hartwig JH, Stossel TP. 2014. Documentation and  
828 localization of force-mediated filamin A domain perturbations in moving  
829 cells. *Nat Commun* 5:4656. <https://doi.org/10.1038/ncomms5656>.
- 830 43. Pentikainen U, Ylanne J. 2009. The regulation mechanism for the auto-  
831 inhibition of binding of human Filamin A to integrin. *J Mol Biol* 393:644-657.  
832 <https://doi.org/10.1016/j.jmb.2009.08.035>.
- 833 44. Becavin C, Bouchier C, Lechat P, Archambaud C, Creno S, Gouin E, Wu Z,  
834 Kuhbacher A, Brisse S, Pucciarelli G, Garcia-del Portillo F, Hain T, Portnoy  
835 DA, Chakraborty T, Lecuit M, Pizarro-Cerda J, Mozner, I, Bierne, H, Cossart

- 836 P. 2014. Comparison of widely used *Listeria monocytogenes* strains EGD,  
837 EGDe, 10403S, and EGD-e highlights genomic differences underlying  
838 variations in pathogenicity. *mBio* 5:e00969-14.  
839 <https://doi.10.1128/mBio.00969-14>
- 840 45. Nichols CD, Casanova JE. 2010. Salmonella-directed recruitment of new  
841 membrane to invasion foci via the host exocyst complex. *Curr Biol* 20:1316-  
842 1320. <https://doi:10.1016/j.cub.2010.05.065>.
- 843 46. Rauch L, Hennings K, Trasak C, Roder A, Schroder B, Koch-Nolte F, Rivera-  
844 Molina F, Toomre D, Aepfelbacher M. 2016. *Staphylococcus aureus* recruits  
845 Cdc42GAP through recycling endosomes and the exocyst to invade human  
846 endothelial cells. *J Cell Sci* 129:2937-2949.  
847 <https://doi.org/10.1242/jcs.186213>.
- 848 47. Ireton K, Van Ngo H, Bhalla M. 2018. Interaction of microbial pathogens with  
849 host exocytic pathways. *Cell Microbiol* 20:e12861. [https://doi.org/doi:](https://doi.org/doi:10.1111/cmi.12861)  
850 [10.1111/cmi.12861](https://doi.org/doi:10.1111/cmi.12861).
- 851 48. Dramsi S, Biswas I, Maguin E, Braun L, Mastroeni P, Cossart P. 1995. Entry  
852 of *Listeria monocytogenes* into hepatocytes requires expression of InIB, a  
853 surface protein of the internalin multigene family. *Mol Microbiol* 16:251-261.  
854 <https://doi.org/https://10.1111/j.1365-2958.1995.tb02297.x>.
- 855 49. Basar T, Shen Y, Ireton K. 2005. Redundant roles for Met docking site  
856 tyrosines and the Gab1 pleckstrin homology domain in InIB-mediated entry of  
857 *Listeria monocytogenes*. *Infect Immun* 73:2061-2074.  
858 <https://doi.org/10.1128/IAI.73.4.2061-2074.2005>.
- 859 50. Jiwani S, Wang Y, Dowd GC, Gianfelice A, Pichestapong P, Gavicherla B,  
860 Vanbennekorn N, Ireton K. 2012. Identification of components of the type IA

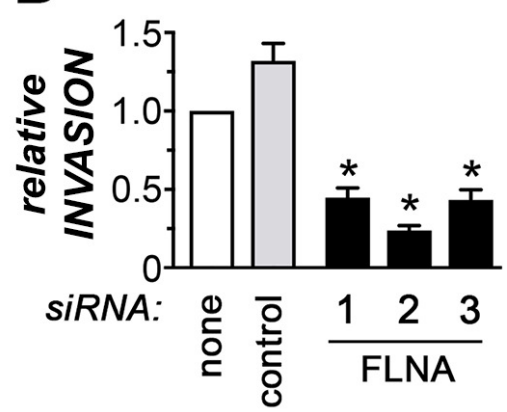
- 861 phosphoinositide 3-kinase pathway that promote internalization of *Listeria*  
862 *monocytogenes*. *Infect Immun* 80:1252-1266. [https://doi.org/](https://doi.org/10.1128/IAI.06082-11)  
863 [10.1128/IAI.06082-11](https://doi.org/10.1128/IAI.06082-11).
- 864 51. Gianfelice A, Le PH, Rigano LA, Saila S, Dowd GC, McDivitt T,  
865 Bhattacharya N, Hong W, Stagg SM, Ireton K. 2015. Host endoplasmic  
866 reticulum COPII proteins control cell-to-cell spread of the bacterial pathogen  
867 *Listeria monocytogenes*. *Cell Microbiol* 17:876-892.  
868 <https://doi.org/10.1111/cmi.12409>.

# Figure 1

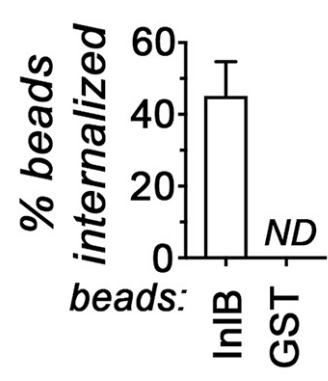
## A



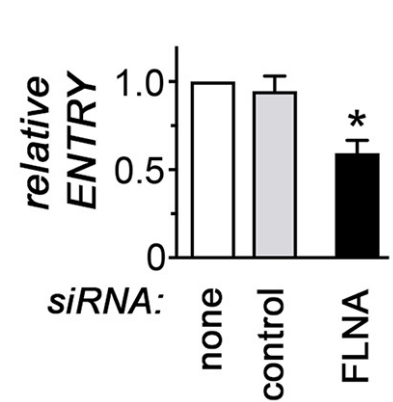
## B



## C (i)

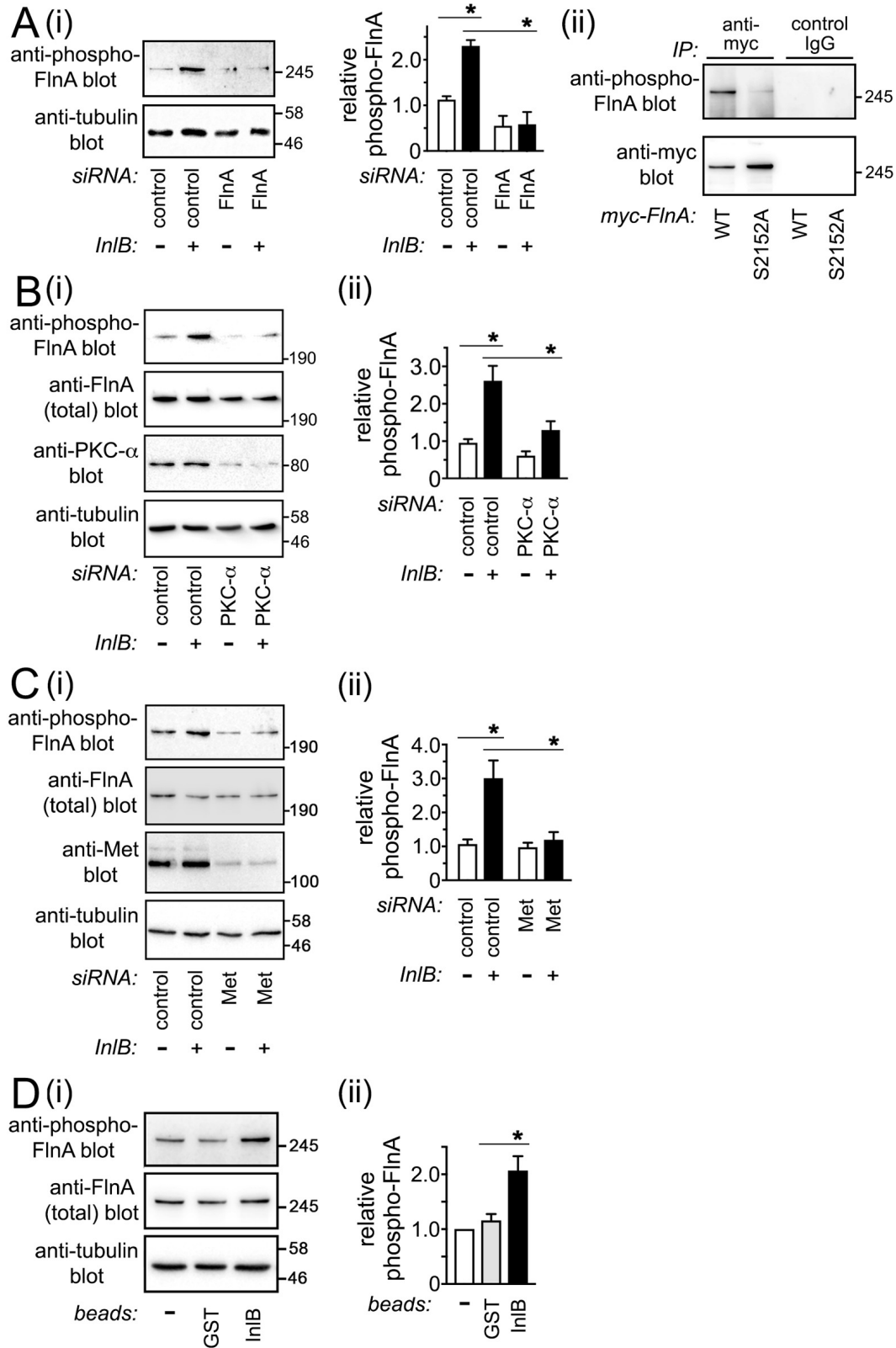


## (ii)





## Figure 2



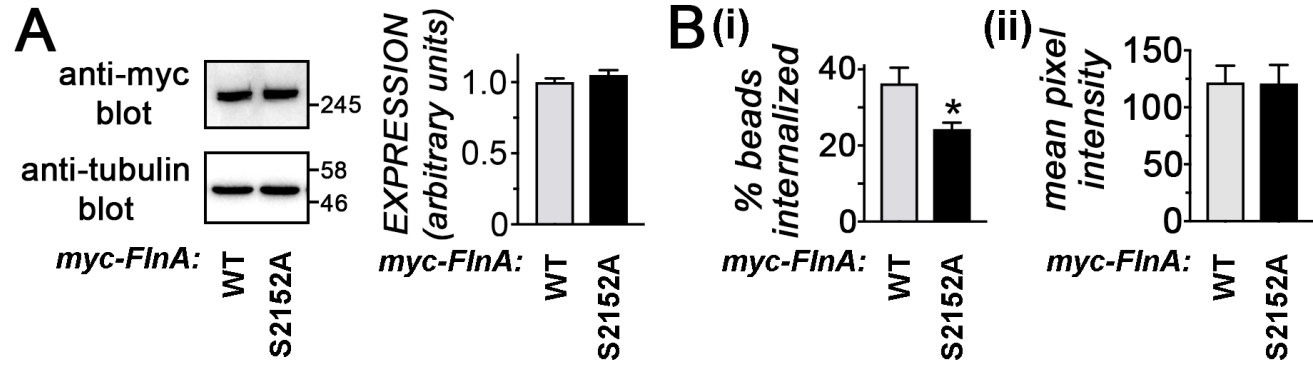
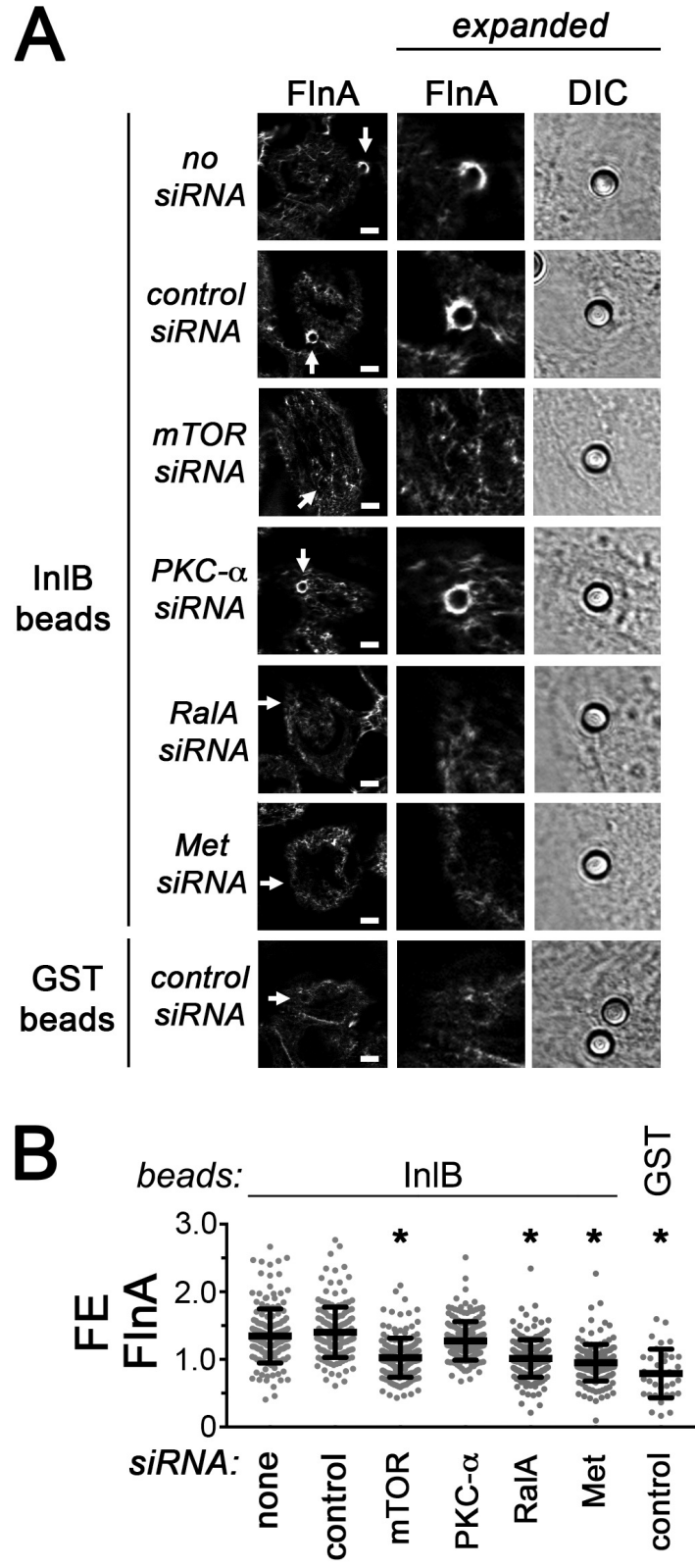
**Figure 3**

Figure 4



**Figure 5**

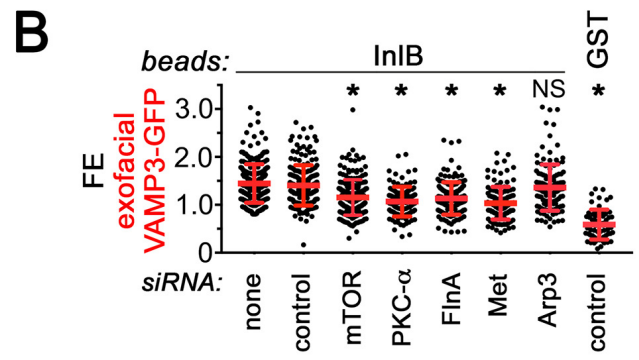
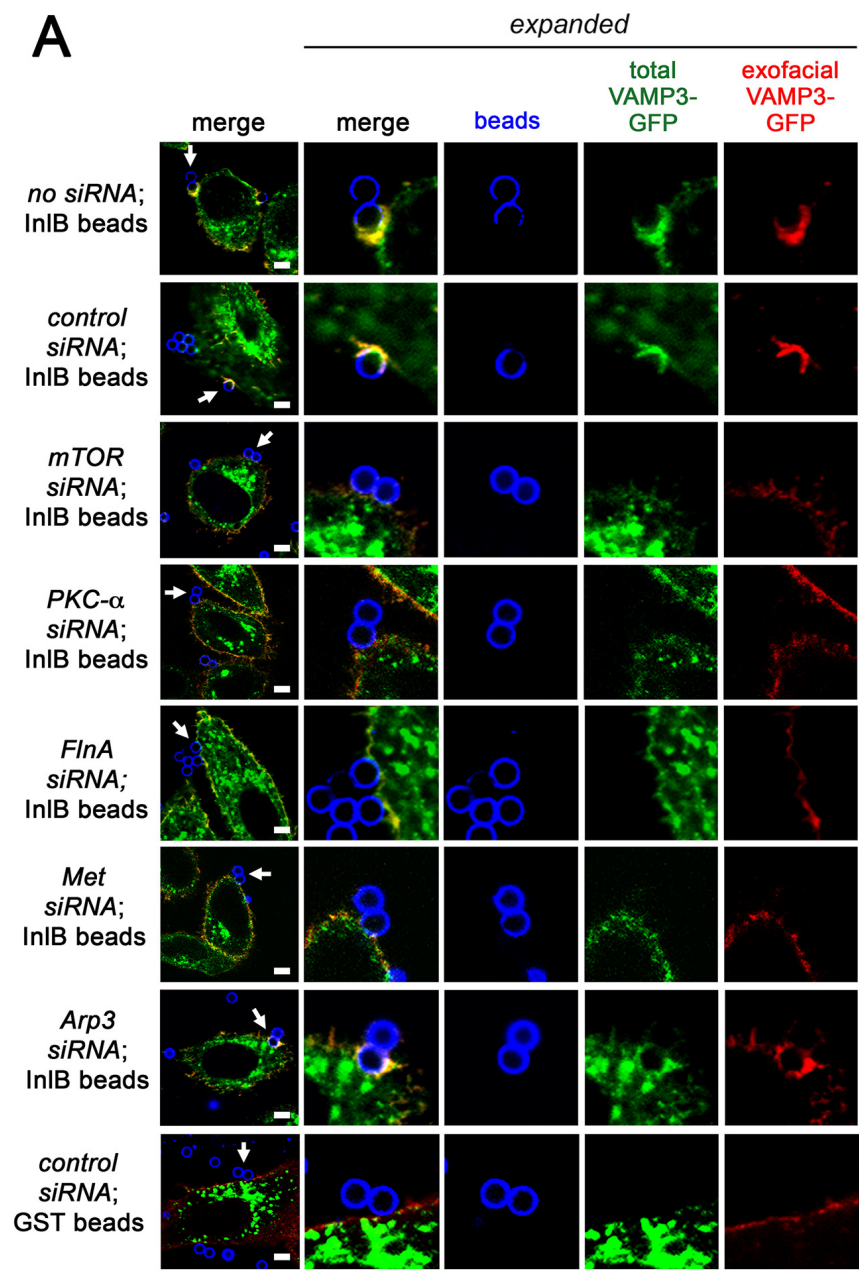
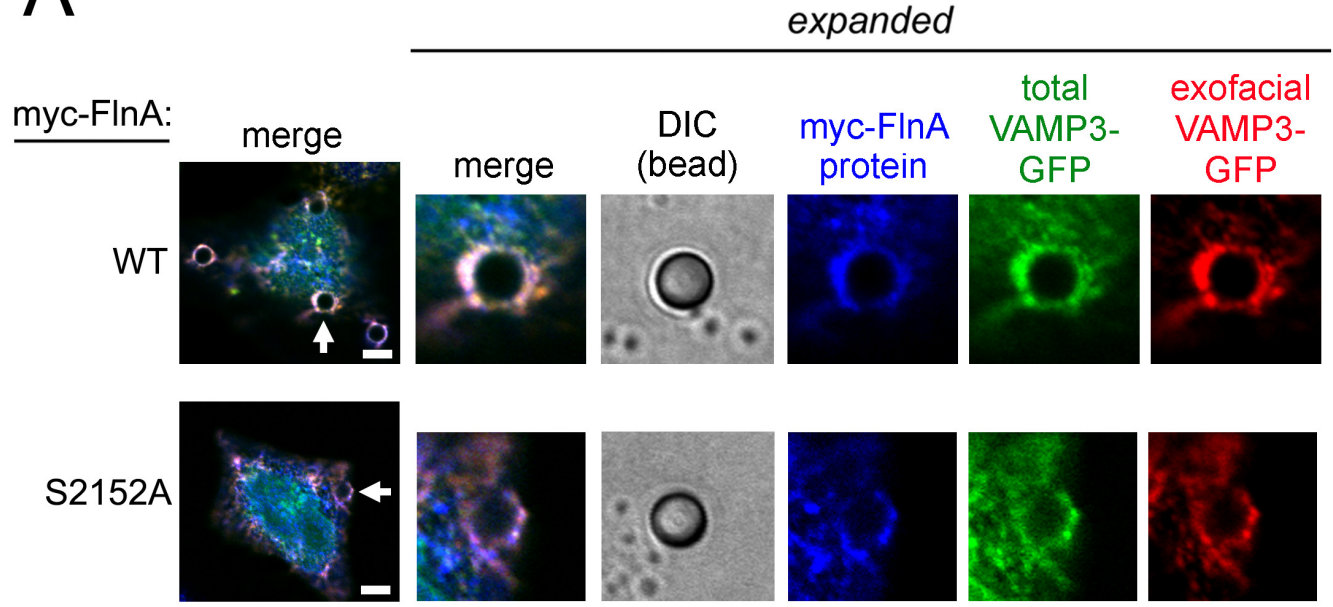
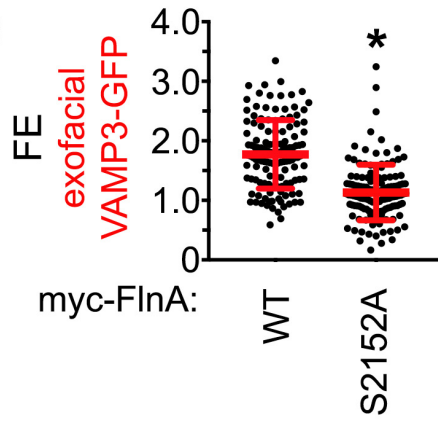


Figure 6

A



B (i)



(ii)

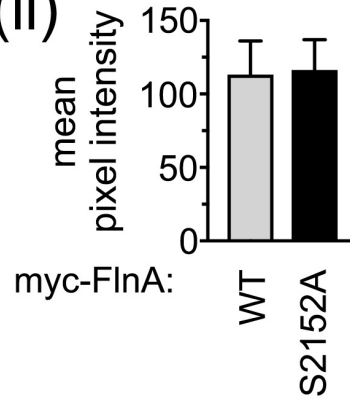


## Figure 7

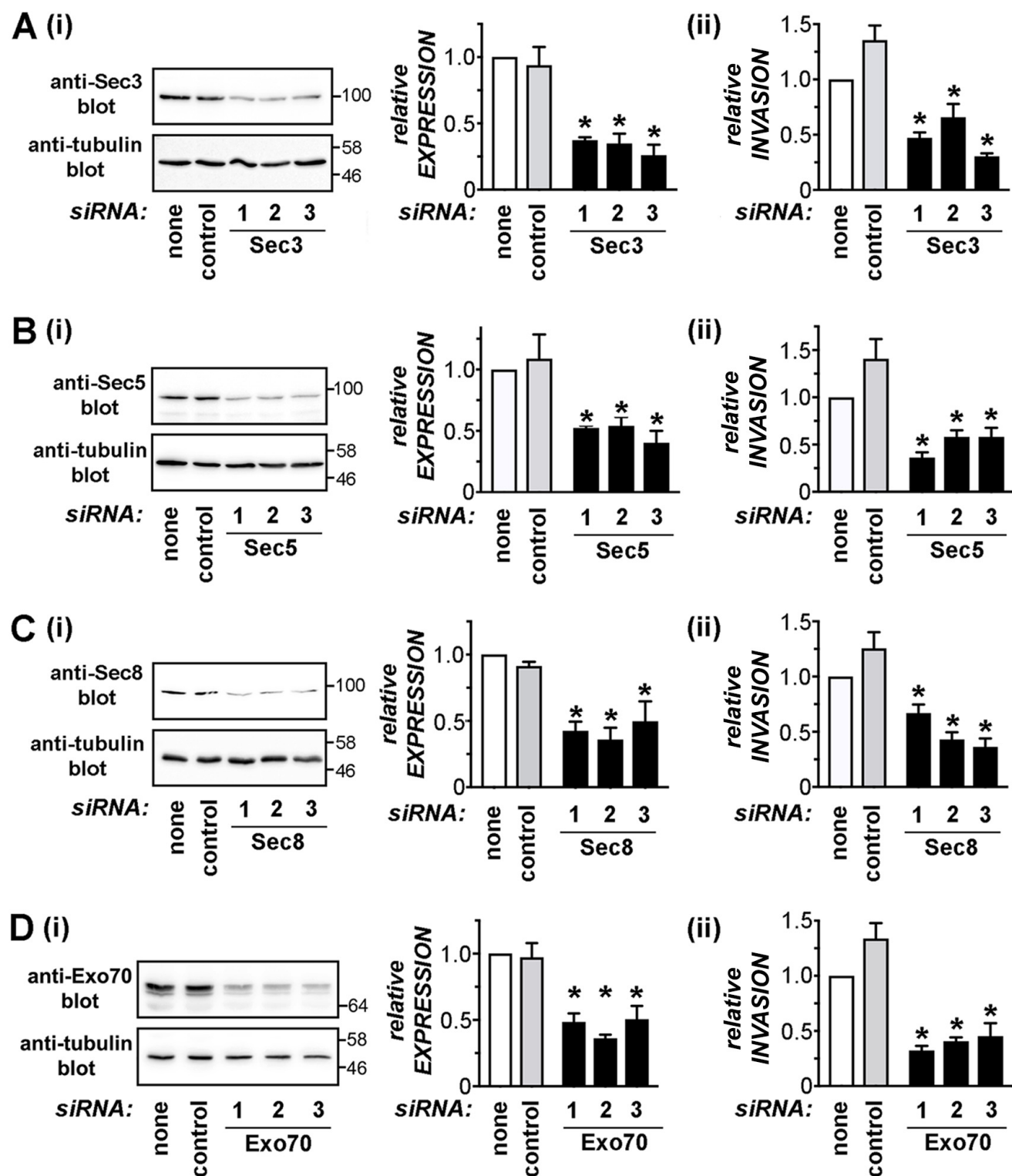




Figure 8

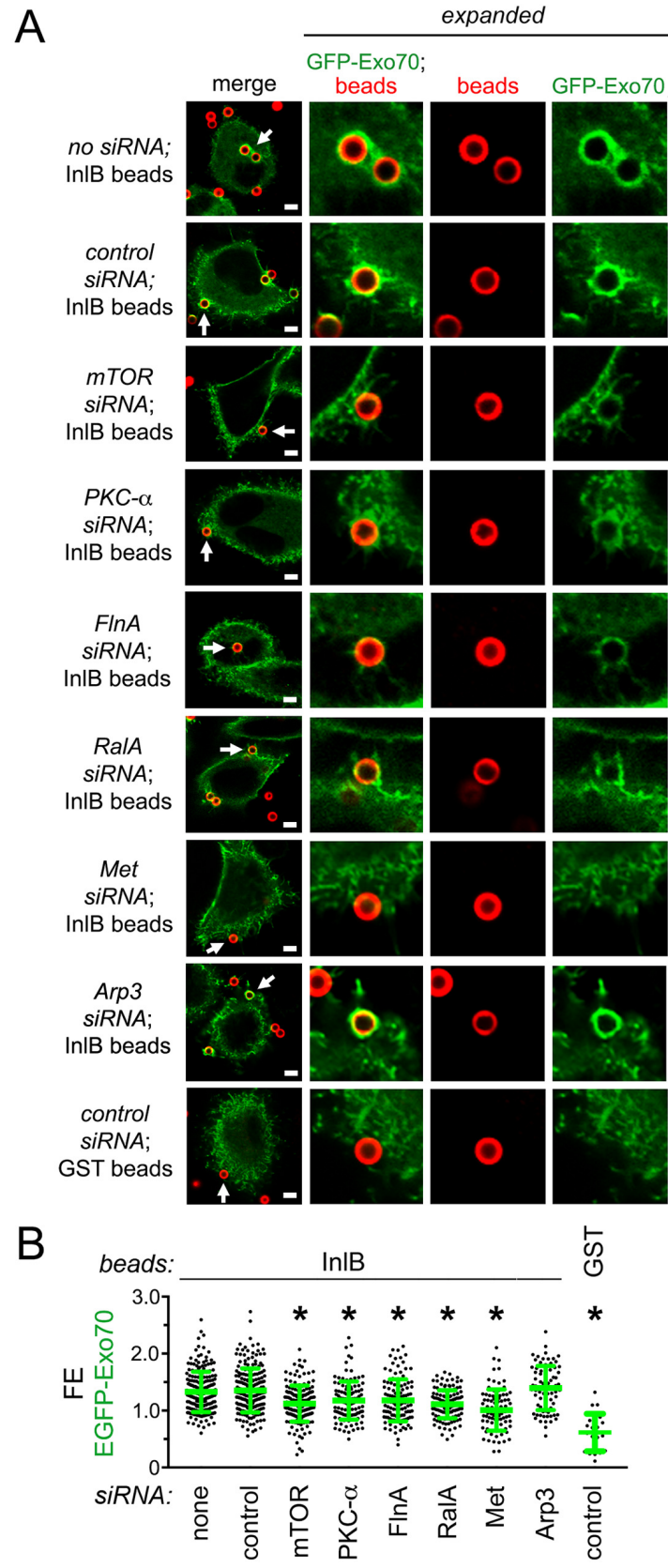


Figure 9

